Eur. Phys. J. D **11**, 31–36 (2000)

THE EUROPEAN PHYSICAL JOURNAL D

EDP Sciences

Positron impact ionisation of He^+ ion

B. Nath[1], S. Chattopadhyaya[2], and C. Sinha[2,a]

[1] Kumar Ashutosh Institution (Main) Boys' 10/1, Dum Dum Road, Calcutta-700 030, India
[2] Department of Theoretical Physics, Indian Association for the Cultivation of Science, Jadavpur, Calcutta-700 032, India

Received 10 July 1999 and Received in final form 7 December 1999

Abstract. Triple differential cross-sections (TDCS) of a hydrogenic (He^+) ion has been studied by positron impact using coplaner geometry for both symmetric and asymmetric kinematics in the intermediate and medium high incident energy region. TDCS has also been studied of He^+ ion by electron impact for symmetric kinematics taking account of the electron exchange effect. The final state wavefunction is chosen as the correlated 3-body Coulomb wavefunction satisfying the exact asymptotic boundary condition. The long range Coulomb interaction in the initial channel between the ionic target and the projectile has also been taken into account properly. For positron impact, the collision is found to be almost recoilless at lower incident energies, in contrast to the strong recoil peak noted in the case of electron impact ionisation. For electron impact, the exchange effect is found to be significantly high for equal energy sharing in the final channel.

PACS. 34.80.Dp Atomic excitation and ionization by electron impact

1 Introduction

Ionisation of atoms and ions by electron and positron impact has created increasing interest among the theoretical and experimental workers. During the last two decades energy and angular distributions of secondary electrons ejected in ionising collisions have been studied exhaustively for electron-atom collisions, while for ionic targets the available data are so long limited to total ionisation cross-sections only. However because of severe intensity limitations, experiments on positron-atom ionisation are far behind the corresponding electron experiments. Recently the technological progress for the production of intense beam of moderate and energy resolved positrons indicates the bright future for the possibility of carrying out parallel experimental studies with positron impact as well. In fact a few experiments have been performed by different experimental groups [1–4] on the measurement of total ionisation cross-sections of some neutral atoms (*e.g.* hydrogen, helium) by positron impact. However, no experimental data is yet available for positron impact ionisation of any ionic target. Further, the triple differential cross-section (TDCS) measurement which provides the most complete and detailed informations for single ionisation process is not yet accessible experimentally by positron impact even for atomic targets. One of the major goal of scattering experiments with positron as projectile, is the comparison of the positron data with the corresponding electron scattering data in order to improve the understanding of the electron-atom/ion interactions.

[a] e-mail: tpcs@mahendra.iacs.res.in

Theoretically, the difference of the scattering cross-sections by positron and electron impact arises solely from higher order calculation since the first Born cross-section does not depend on the sign of the projectile charge. Hence, the charge asymmetry for the particular process (*e.g.* ionisation) which gives direct information of the effect of higher order interaction can be studied through the comparison of electron and positron results. In the absence of any experiment, the theoretical study of the TDCS should therefore provide some guideline of the detailed informations for a particular ionisation process. Further, since for e^+ impact, the scattered projectile and the ejected electron are distinguishable unlike the case of electron impact, the absence of electron exchange effect makes the system ideal for the study of the electrostatic interactions between the outgoing particles. In contrast, for electron impact ionisation, such study is difficult since the effect of correlation between the outgoing electrons is masked by the electron exchange.

From the physical point of view, the basic difference between the electron and the positron impact collision, particularly in the low and intermediate energy region is that in the former the effect of electron exchange needs to be taken into account while in the latter, the Ps formation channel plays a very important role and should be incorporated in a theoretical model [5].

Recently we developed an approach [6] to calculate the TDCS of fast electron impact ionisation of a hydrogenic ion (He^+) for asymmetric geometry where the final state wavefunction satisfies proper asymptotic boundary condition for an ionisation process, by choosing the correlated

three body coulomb continuum. In the present work we have extended our previous [6] method to calculate the TDCS for fast positron impact ionisation of (He^+)-ion for both symmetric and asymmetric geometries. The correlated coulomb continuum in the present case (*i.e.* for e^+ impact ionisation) also accounts for the effect of Ps formation in the continuum state (ECC) which can be thought of as another mechanism of indirect ionisation. Now, single ionisation of He^+ by e^+ impact can take place by the following reactions:

$$e^+ + He^+ \rightarrow e^+ + He^{++} + e^-, \quad \text{(A1)}$$

$$e^+ + He^+ \rightarrow Ps + He^{++}. \quad \text{(A2)}$$

Since the present study which deals with reaction (A1) concentrates mainly on high energy region, the effect of Ps formation channel is not supposed to play any important role and the present model does not take account of this. The long range coulomb repulsion occurring in the initial channel between the incident positron and the target ion (He^+) has been properly taken into account in the framework of Coulomb Born Approximation where the incident positron is represented by a coulomb continuum wave. To our knowledge, no attempt has yet been made to study the TDCS of an ionic target by positron impact. We have also studied here the TDCS of He^+ ion by electron impact for symmetric kinematics incorporating the electron exchange effect, which we neglected in our earlier work [6].

Due to inadequacy of measurements, theoretical works on positron impact ionisation are much limited in the literature as compared to the works on electron impact ionisation. For ionic (positive) targets, there exist some models applied to the electron impact ionisation in both high and low energy regime. Of the low energy theoretical models, different versions of R-Matrix methods [7–9] and the usual Close-Coupling [10] approximation are worthy to be mentioned. All these models have been applied to calculate the total ionisation cross-sections and in few cases single differential cross-sections [11,12] of some complex positive ions by electron impact in the low/intermediate energy region. Particularly in the R-Matrix approach developed by Burke *et al.* [11–13] and later applied by other authors [14], the distorted wave theory and the close-coupling approach have been combined to describe the "fast" (ionising) and the "slow" (ejected) electron respectively. This approach has been found to give more or less good agreement with the experiments for electron impact ionisation of positive ions in the low/intermediate energy region.

2 Theory

The prior form of the T-matrix element for $e^{\pm}$–He^+ ionisation process is given by

$$T_{\rm if} = \langle \Psi_{\rm f}^- | V_{\rm i} | \psi_{\rm i} \rangle. \quad (1)$$

The total Hamiltonian of the system is written as

$$H = H_0 \pm \frac{Z_{\rm t}}{r_1} \mp \frac{1}{r_{12}} \quad (2)$$

where the upper sign refers to the e^+ impact while the lower sign stands for e^- impact. $Z_{\rm t}(=2)$ being the charge of the target nucleus; $\mathbf{r}_1$ and $\mathbf{r}_2$ are the position vectors of the incident $e^{\pm}$ "1" and the bound electron "2" respectively, with respect to the target nucleus; $\mathbf{r}_{12} = \mathbf{r}_1 - \mathbf{r}_2$; H_0 in equation (2) is the full kinetic energy operator given by

$$H_0 = -\frac{1}{2}\nabla_1^2 - \frac{1}{2}\nabla_2^2.$$

The initial wavefunction $\psi_{\rm i}$ in equation (1) satisfies the equation

$$\left[H_0 - \frac{Z_{\rm t}}{r_2} \pm \frac{Z_{\rm t}-1}{r_1}\right]\psi_{\rm i} = E_0\psi_{\rm i} \quad (3)$$

where

$$\psi_{\rm i} = (2\pi)^{-3/2} \exp\left(\frac{1}{2}\pi\alpha_{\rm i}\right) \Gamma(1 - {\rm i}\alpha_{\rm i}) \times \exp({\rm i}\mathbf{k}_{\rm i}\cdot\mathbf{r}_1)\,{}_1F_1[{\rm i}\alpha_{\rm i}, 1; {\rm i}(k_{\rm i}r_1 - \mathbf{k}_{\rm i}\cdot\mathbf{r}_1)]\phi_{\rm i}(\mathbf{r}_2, \mathbf{r}_3),$$

with $\alpha_{\rm i} = \pm(Z_{\rm t}-1)/k_{\rm i}$ and $E_0 = k_{\rm i}^2/2 + \varepsilon_{\rm i} = E_{\rm i} + \varepsilon_{\rm i}$, $\mathbf{k}_{\rm i}$ being the initial momentum of the incident $e^{\pm}$, $\varepsilon_{\rm i}$ is the binding energy and $\phi_{\rm i}$ is the bound state wavefunction of the ground state of the hydrogenic ion

$$\phi_{\rm i}(\mathbf{r}_2, \mathbf{r}_3) = \frac{Z_{\rm t}^{3/2}}{\sqrt{\pi}} \exp\left(-\lambda_{\rm i} r_2\right) \quad (4)$$

$\lambda_{\rm i}$ being the bound state parameter of the ground state of the hydrogenic ion. Thus from equations (1–4), the interaction in the initial channel is obtained as

$$V_{\rm i} = \pm\frac{1}{r_1} \mp \frac{1}{r_{12}}\cdot \quad (5)$$

It is evident from equation (5) that the perturbation $V_{\rm i}$ vanishes asymptotically (for $\mathbf{r}_1 \rightarrow \infty$ and $\mathbf{r}_2$ finite).

The final state wavefunction $\Psi_{\rm f}^-$ in equation (1) is an exact solution of the three body problem satisfying the incoming wave boundary condition, *i.e.* $\Psi_{\rm f}^-$ satisfies the equation

$$(H - E)\Psi_{\rm f}^- = 0. \quad (6)$$

For the prescription of the final state wavefunction $\Psi_{\rm f}^-$, the correlated 3-body coulomb continuum is chosen [5];

$$\Psi_{\rm f}^-(\mathbf{r}_1, \mathbf{r}_2) = C \exp({\rm i}\mathbf{k}_1\cdot\mathbf{r}_1)\,{}_1F_1[{\rm i}\alpha_1, 1; -{\rm i}(k_1 r_1 + \mathbf{k}_1\cdot\mathbf{r}_1)] \times \exp({\rm i}\mathbf{k}_2\cdot\mathbf{r}_2)\,{}_1F_1[{\rm i}\alpha_2, 1; -{\rm i}(k_2 r_2 + \mathbf{k}_2\cdot\mathbf{r}_2)] \times {}_1F_1[{\rm i}\alpha_{12}, 1; -{\rm i}(k_{12} r_{12} + \mathbf{k}_{12}\cdot\mathbf{r}_{12})] \quad (7)$$

where the constant C is given by

$$C = (2\pi)^{-3} \exp\left[-\frac{1}{2}\pi(\alpha_1 + \alpha_2 + \alpha_{12})\right] \times \Gamma(1 - {\rm i}\alpha_1)\Gamma(1 - {\rm i}\alpha_2)\Gamma(1 - {\rm i}\alpha_{12})$$

with $\alpha_1 = \pm 2/|\mathbf{k}_1|$, $\alpha_2 = -2/|\mathbf{k}_2|$, $\alpha_{12} = \mp 1/2|\mathbf{k}_{12}|$, $\mathbf{k}_{12} = (\mathbf{k}_1 - \mathbf{k}_2)/2$; $\mathbf{k}_{\rm i}$, $\mathbf{k}_1$ denote the momentum of the incident and scattered positron/electron while $\mathbf{k}_2$ stands for the momentum of the ejected electron.

For electron impact ionisation, the exchange amplitude $(\mathbf{k}_1, \mathbf{k}_2)$ can be obtained by interchanging $\mathbf{k}_1$ and $\mathbf{k}_2$ in the expression for the direct amplitude;

$$g(\mathbf{k}_1, \mathbf{k}_2) = f(\mathbf{k}_2, \mathbf{k}_1) \tag{8}$$

where

$$f(\mathbf{k}_1, \mathbf{k}_2) \equiv T_{\rm if}(\mathbf{k}_1, \mathbf{k}_2).$$

Finally the expression for the TDCS by e^+ impact is given by

$$\frac{\mathrm{d}^3\sigma}{\mathrm{d}E_2 \mathrm{d}\Omega_1 \mathrm{d}\Omega_2} = (2\pi)^4 \frac{k_1 k_2}{k_{\rm i}} |f|^2 \tag{9a}$$

while the expression for the TDCS by e^- impact (with exchange) is given by

$$\frac{\mathrm{d}^3\sigma}{\mathrm{d}E_2 \mathrm{d}\Omega_1 \mathrm{d}\Omega_2} = (2\pi)^4 \frac{k_1 k_2}{k_{\rm i}} \left[\frac{1}{4}|f+g|^2 + \frac{3}{4}|f-g|^2\right]. \tag{9b}$$

The ionisation amplitude f, g in equations (9a, 9b) contains four coulomb wavefunctions which make the analysis as well as computation much involved. After analytic reduction [6], the T-matrix element finally requires the evaluation of a three-dimensional integration to be performed numerically [15,16].

3 Results and discussion

We have computed the TDCS for ionisation of a singly ionised helium atom (He^+) in its ground state by positron impact (Figs. 1–10) in a coplanar geometry for intermediate and medium high incident energies, *e.g.*, $E_{\rm i}$ = 100, 250, 354.4, 500 and 1000 eV. Special emphasis

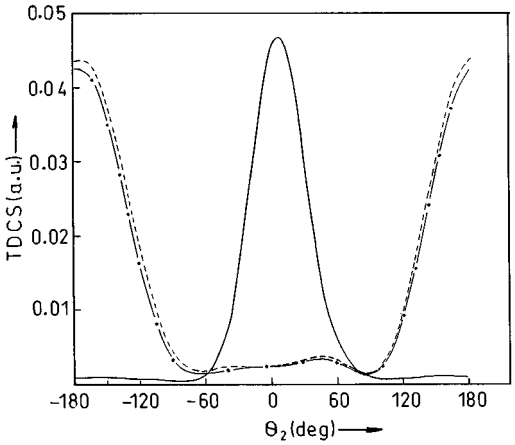

Fig. 1. The TDCS in atomic units (a.u.) for the ionisation of He^+ ion from the ground state 1S by positron and electron impact for the case, incident energy $E_{\rm i}$ = 100 eV, ejected energy E_2 = 5 eV, and scattering angle $\theta_1 = 4^\circ$, as a function of angle θ_2. Solid curve for positron impact; dashed curve for electron impact (without exchange) and long dashed-dot curve for electron impact with exchange effect.

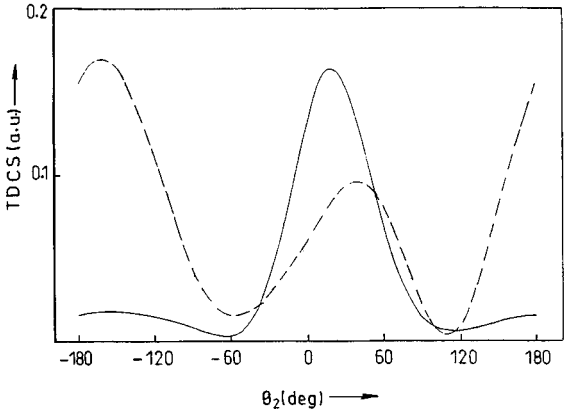

Fig. 2. The TDCS in atomic units (a.u.) for the ionisation of He^+ ion from the ground state 1S by positron and electron impact for the case, $E_{\rm i}$ = 250 eV, E_2 = 5 eV, and $\theta_1 = 4^\circ$, as a function of θ_2. Solid curve for positron impact and dashed curve for electron impact.

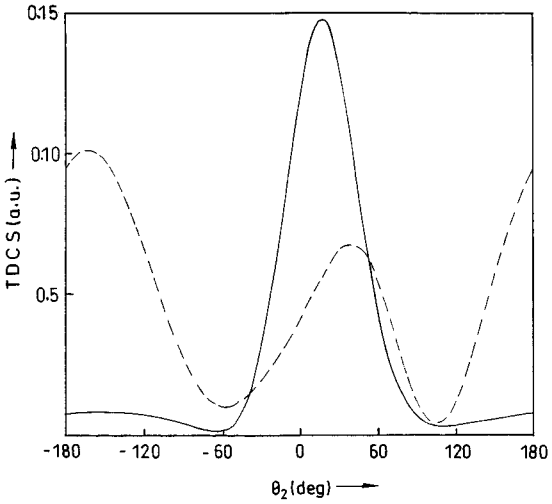

Fig. 3. Same as Figure 2 with E_2 = 10 eV.

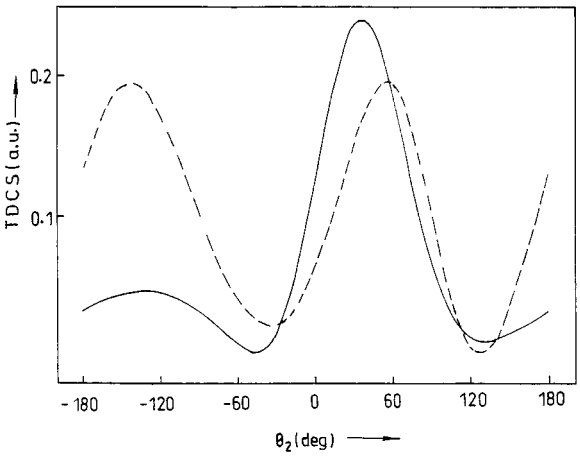

Fig. 4. Same as Figure 2 with $E_{\rm i}$ = 500 eV.

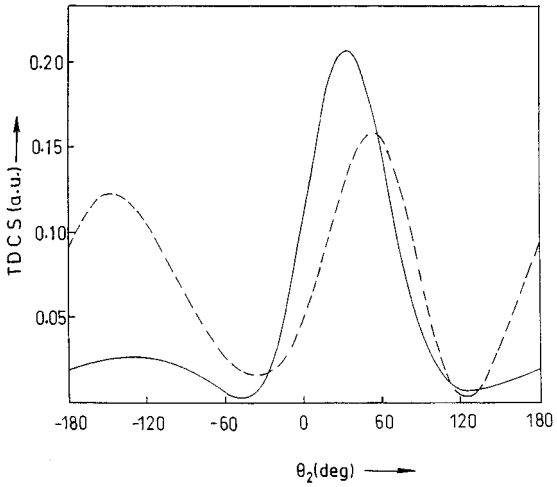

Fig. 5. Same as Figure 4 with $E_2 = 10$ eV.

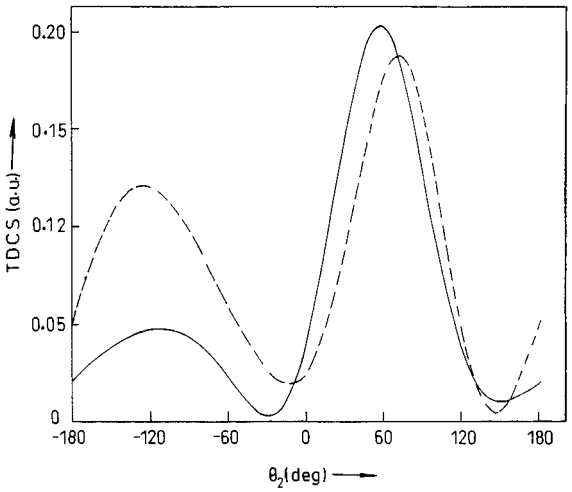

Fig. 6. Same as Figure 2 with $E_i = 1000$ eV.

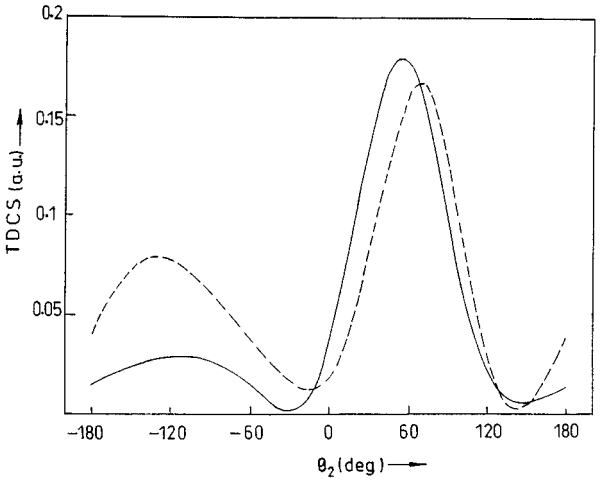

Fig. 7. Same as Figure 6 with $E_2 = 10$ eV.

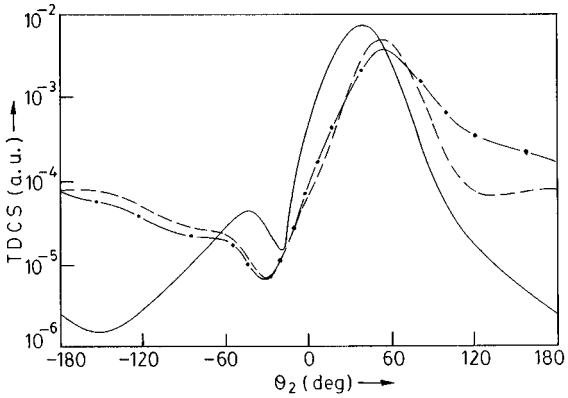

Fig. 8. Same as Figure 1 with $E_i = 354.4$ eV, $E_2 = 100$ eV and $\theta_1 = 30°$.

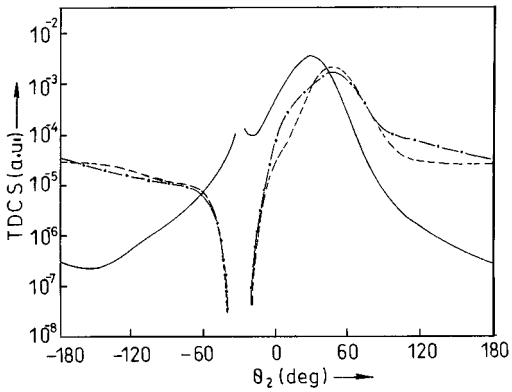

Fig. 9. The TDCS in atomic unit (a.u.) for the ionisation of the He^+ ion from the ground state 1S by positron and electron impact for symmetric kinematics at $E_i = 354.4$ eV; $E_2 = 150$ eV and $\theta_1 = 30°$, as a function of angle θ_2. Solid curve for positron impact; dashed curve for electron impact (without exchange) and long dashed-dot curve for electron impact with exchange effect.

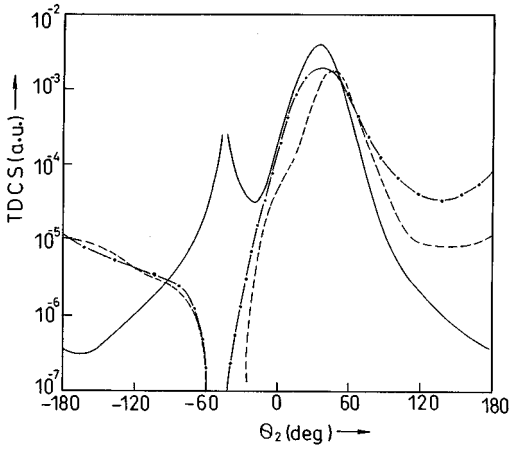

Fig. 10. Same as Figure 9 with $\theta_1 = 45°$.

has been given on the asymmetric geometry for e^+ impact, although some TDCS results have been presented for symmetric and near-symmetric geometries as well. We have also computed the TDCS results for e^- impact for some symmetric kinematics only since the results for asymmetric kinematics has already been reported earlier [5]. In the present calculation for e^- impact, the electron exchange effect has been incorporated which was neglected in our previous work [5]. In order to show the charge dependence of the TDCS, we compare the results for positron and electron impact in all the figures (Figs. 1–10).

Figures 1–7 demonstrate a comparative study between the TDCS of e^+ and e^- impact ionisation for asymmetric kinematics (*i.e.* when the ejected and the scattered particles share widely unequal energies) at incident energies E_i = 100, 250, 500 and 1000 eV and ejected energies E_2 = 5 and 10 eV, for fixed scattering angle 4°. Figures 1–7 show an intense binary peak for e^+ impact in contrast to the intense recoil peak for electron impact ionisation. Particularly at lower incident energies, for e^+ impact (vide Figs. 1–5), the collision is mainly binary *i.e.* almost recoilless while for e^- impact the intensity of the recoil peak is even larger than the binary one. However with increasing incident energy, (see Figs. 6 and 7) the recoil peak becomes more and more prominent for e^+ impact (as compared to the lower incident energy case) while for e^- impact, the converse is true *i.e.* the magnitude of the recoil peak decreases and the intensity of the binary peak finally takes over with increasing incident energy.

Figures 2–7 also indicate that, as the ejected energy E_2 increases, both the binary and the recoil peak intensities decrease for positron as well as electron impact. Further, it is evident from Figures 1, 2, 4 and 6 that for both $e^{\pm}$ impact, the position of the binary peak is shifted towards higher ejection angle with increasing incident energy (*e.g.* for e^+ impact, 5° for 100 eV, 16° for 250 eV, 36° for 500 eV and 56° for 1000 eV), whereas for the corresponding recoil peak, it is shifted towards smaller angle (*e.g.* 160° for 100 eV, 150° for 250 eV, 130° for 500 eV and 110° for 1000 eV). However, with increasing ejected energy, while keeping the incident energy fixed, both the binary and recoil peak positions remain almost the same. This behaviour is also true for both e^+ and e^- impact.

The difference between the electron and positron TDCS gets smaller and smaller with increasing incident energy, as is expected physically. It is also noted from Figures 1–7 that the positions of both the binary and recoil peaks for the e^+ impact occurs at smaller ejection angles than the corresponding electron peaks.

Since for asymmetric geometry, the velocities of the two outgoing electrons in case of e^- impact, are quite apart, the effect of electron exchange in the TDCS result is not very significant and as such we have compared the direct and exchange results for only one asymmetric kinematics for very low incident energy *e.g.*, E_i = 100 eV, where the exchange effect is supposed to give some reasonable contribution (vide Fig. 1). As may be noted from Figure 1 the exchange cross-section is always lower than the direct one.

Figure 8 represents the electron and positron impact data for E_i = 354.4 eV, E_2 = 100 eV and θ_1 = 30°. It shows that in the near-symmetric region (*i.e.* when the outgoing particles share almost equal energy) the nature of the positron and electron curves differ appreciably than the curves for highly asymmetric geometries. For this geometry (near symmetric), there is a structural dissimilarity between the electron and positron curve in the recoil region. For e^+ impact a small but distinct recoil peak appears at around $\theta_2 \simeq 42°$ while for e^- impact no such distinct recoil peak exists except for some wavy structures. Figure 8 also reveals that in the recoil region, a maxima of the e^- curve corresponds to a minima of the e^+ curve and *vice versa*, which is expected physically. It is also noted that as we move more and more towards symmetric geometry (not shown in the figures) the magnitude of the recoil peak of the e^+ curve is increasingly enhanced while in contrast, the minima of the corresponding e^- curve gets more and more deep. In fact, the positron-electron/electron-electron interaction in the final channel is responsible (physically) for such behaviour. Regarding the electron exchange effect, it may be noted from Figure 8 that in the near symmetric kinematics, the exchange effect reduces the cross-section in the recoil region while in the binary region, except near the peak ($\sim 26°-74°$), it enhances the cross-section. In fact in both the recoil and binary regions the exchange effect is found to be more prominent for large ejection angles.

Figure 9 displays the triple differential cross-sections when the scattered positron/electron and the ejected electron share identical energy in the final channel (*e.g.* E_i = 354.4 eV, θ_1 = 30° and $E_1 = E_2$ = 150 eV). As may be noted from the figure, for e^+ impact, the differential cross-section shows singular structure when the scattered positron and the ionised electron emerge in the same direction. This behaviour may be physically explained as arising due to the process of electron capture to the continuum (ECC). In fact for positron impact, the ionisation cross-section diverges as the inverse of the relative velocity between the incident positron and the emerging electron and from the mathematical point of view, this divergence occurs due to the Coulomb density of states factor (vide Eq. (7)) involving the electron positron correlation term (attractive). In contrast, for e^- impact, the same Coulomb density of states factor that accounts for the coulomb repulsion between the scattered and ionised electron, gives rise to an exponentially vanishing cross-section (see Fig. 9) when the two out going electrons emerge with equal velocity. The divergence in the cross-section due to the ECC effect is also evident from Figure 10, where we have plotted the results for the same symmetric kinematics but at a fixed scattering angle $\theta_1 = 45°$.

As may be noted from Figures 9 and 10 for equal energy sharing, the exchange effect is mainly appreciable in the binary region. Figure 9 shows that in the binary region, the exchange cross-section is higher than the direct one except near the peak region. In contrast, in the recoil region, the exchange curve lies always below the direct one except at the extreme forward ($\sim 0°-20°$) and extreme

backward angle ($\sim 170°-180°$). In Figure 10 also, the exchange effect enhances the cross-section in the binary region except between the crossing points of the direct and exchange curve ($\sim 50°-70°$). In the recoil region however, the effect of exchange is not very significant as compared to the binary region. In this region also the exchange curve lies above the direct one for ejection angles up to 120° where the two curves (exchange and direct) cross each other. Beyond this crossing, the exchange curve lies below the direct one up to the second crossing at around 175°.

References

1. H. Knudsen, L. Brun-Nielsen, M. Charlton, M.R. Poulsen, J. Phys. B: At. Mol. Opt. Phys. **23**, 3955 (1990).
2. D. Fromme, G. Kruse, W. Raith, G. Sinapius, Phys. Rev. Lett. **57**, 3031 (1986).
3. G.O. Jones, M. Charlton, J. Slevin, G. Laricchia, A. Kover, M.R. Poulsen, S. Nic Chormaic, J. Phys. B: At. Mol. Opt. Phys. **26**, L483 (1993).
4. G. Spicher, B. Olsson, W. Raith, G. Sinapius, W. Sperber, Phys. Rev. Lett. **64**, 1019 (1990).
5. H.R.J. Walters, J.E. Blackwood, C.P. Campbell, M.T. McAlinden, *10th Workshop on Low-Energy Positron and Positronium Physics*, KEK, Tsukuba, Japan, 1999, p. 13.
6. R. Biswas, C. Sinha, J. Phys. B: At. Mol. Opt. Phys. **30**, 1589 (1997).
7. P.G. Burke, D.W. Robb, Adv. At. Mol. Phys., Academic Press **11**, 143 (1975).
8. P.G. Burke, *Physics of electronic and atomic collisions*, edited by S. Datz (North Holland, Amsterdam, 1982), p. 447.
9. P.G. Burke *et al.*, Proc. Roy. Soc. Lond. A **410**, 289 (1987).
10. D.L. Moores, K.J. Reed, Adv. At. Mol. Phys., Academic Press **34**, 301 (1994).
11. K. Laghdas, R.H.J. Reid, C.J. Joachain, P.G. Burke, J. Phys. B: At. Mol. Opt. Phys. **28**, 4811 (1995).
12. K. Laghdas, R.H.J. Reid, C.J. Joachain, P.G. Burke, J. Phys. B: At. Mol. Opt. Phys. **32**, 1439 (1999).
13. P.G. Burke, A.E. Kingston, A. Thompson, J. Phys. B: At. Mol. Opt. Phys. **16**, L385 (1983).
14. S.S. Tayal, Phys. Rev. A **49**, 2561 (1994).
15. R. Biswas, C. Sinha, Phys. Rev. A **50**, 354 (1994).
16. R. Biswas, C. Sinha, J. Phys. B: At. Mol. Opt. Phys. **28**, 1311 (1995).